

First-principles electron dynamics simulation for optical breakdown of dielectrics under an intense laser field

T. Otobe and M. Yamagiwa

Advanced Photon Research Center, Japan Atomic Energy Agency, Kizugawa, Kyoto 619-0215, Japan

J.-I. Iwata, K. Yabana, and T. Nakatsukasa*

Institute for Physics and Center for Computational Sciences, University of Tsukuba, Tsukuba 305-8571, Japan

G. F. Bertsch

Department of Physics and Institute for Nuclear Theory, University of Washington, Seattle, Washington 98195, USA

(Received 20 February 2008; published 2 April 2008)

We present a first-principles calculation for an optical dielectric breakdown in a diamond, which is induced by an intense laser field. We employ the time-dependent density-functional theory by solving the time-dependent Kohn–Sham equation in real time and real space. For low intensities, the ionization agrees well with the Keldysh formula. The calculation shows a qualitative change of electron dynamics as the laser intensity increases, from dielectric screening at low intensities to optical breakdown at and above 7×10^{14} W/cm². Following the pulse, the electrons excited into the conduction band exhibit a coherent plasma oscillation that persists for tens of femtoseconds.

DOI: [10.1103/PhysRevB.77.165104](https://doi.org/10.1103/PhysRevB.77.165104)

PACS number(s): 78.47.-p, 42.65.Re, 71.15.Mb, 77.90.+k

The interaction of ultrashort laser pulses with dielectrics has been a subject of intense study for both the fundamental interest and possible applications.^{1–9} The key physical process in the interaction is the optical breakdown of the medium creating many electron-hole pairs. This is a highly nonlinear optical process whose mechanism is not fully understood yet.¹⁰ The optical breakdown causes a highly reproducible structure modification of the dielectric, making the process quite suitable for micromachining, medical surgery, and other technical applications.^{4,7,9}

A number of quite different mechanisms have been proposed for the optical breakdown. Electron avalanching is considered to be a principal mechanism for pulses longer than a picosecond.⁶ For femtosecond pulses, photoionization either by a multiphoton or by a tunneling mechanism is expected to become dominant. Some measurements suggest that the electron avalanche is still significant in the femtosecond regime,^{2,11} while others suggest that the electron impact ionization does not play a role in the femtosecond scale.¹² A theoretical description of the optical breakdown has been achieved by employing empirical models, such as a rate equation for the number of excited electrons,^{1,10,11} a kinetic evolution equation for the distribution function,⁶ and a propagation equation for an electric field envelope.^{8,12}

For isolated atoms and molecules under intense ultrashort laser pulses, a numerical approach solving the time-dependent Schrödinger equation is useful.^{13–15} However, to our knowledge, the first-principles computational approach has not been applied for the electron dynamics for bulk systems irradiated by intense ultrashort pulses. In this paper, we report our attempt to describe an optical breakdown of dielectrics based on the time-dependent density-functional theory (TDDFT).¹⁶

The TDDFT combined with the linear response theory has been successfully applied to the optical responses of atoms, molecules, and solids.^{17–20} It has also been used to describe the nonlinear and nonperturbative electron dynamics induced

by intense ultrashort laser pulses.^{21,22} In view of the good experience with TDDFT, we anticipate that it will also provide a useful description of the short-time electron dynamics under an intense ultrashort laser radiation.

The TDDFT is capable of treating the ionization of both multiphoton²¹ and tunneling mechanisms.²³ It also incorporates a dynamical screening effect, which is one of the important many-body correlations. However, since the theory is based on orbitals that only interact through the mean field, effects of electron-electron collisions are not properly taken into account. Thus, the theory is not suited to describe the avalanche mechanism and the TDDFT breakdown threshold should be regarded as the upper limit. We also freeze the ion position in the present calculation so that the thermal relaxation accompanying an energy transfer from electrons to ions is also ignored. The theory is only applicable to the initial excitation of the system before it has had time to thermalize, which is expected to be much longer than the pulse duration.

We apply the TDDFT to a diamond, which is a prototype of a typical insulator. Our computations are performed using a formalism that was originally developed to calculate the dielectric function¹⁹ of crystalline solids. We essentially use the same real-time code to treat the excitation by a laser pulse. By assuming the long wavelength limit and that the pulse laser is represented by a time-dependent spatially uniform electric field $\mathbf{E}_{\text{laser}}(t)$, the electronic motion is described by the following time-dependent Kohn–Sham (TDKS) equation for single-particle orbitals $\psi_i(\mathbf{r}, t)$:

$$i\hbar \frac{\partial}{\partial t} \psi_i(\mathbf{r}, t) = \left\{ \frac{1}{2m} \left(\mathbf{p} + \frac{e}{c} \mathbf{A}_{\text{tot}}(t) \right)^2 + V_{\text{ion}}(\mathbf{r}) + \int d\mathbf{r}' \frac{e^2}{|\mathbf{r} - \mathbf{r}'|} n(\mathbf{r}', t) + \mu_{\text{xc}}(\mathbf{r}, t) \right\} \psi_i(\mathbf{r}, t), \quad (1)$$

where $n(\mathbf{r}, t)$ is the time-dependent density given by $n(\mathbf{r}, t)$

$=\sum_i |\psi_i(\mathbf{r}, t)|^2$, and $\mu_{xc}(\mathbf{r}, t)$ is the exchange-correlation potential. The time-dependent spatially uniform vector potential $\mathbf{A}_{\text{tot}}(t)$ is composed of the external and induced vector potentials, $\mathbf{A}_{\text{tot}}(t) = \mathbf{A}_{\text{ext}}(t) + \mathbf{A}_{\text{ind}}(t)$. The external vector potential $\mathbf{A}_{\text{ext}}(t)$ is related to the electric field of the applied laser pulse, $\mathbf{E}_{\text{laser}}(t) = -d\mathbf{A}_{\text{ext}}(t)/dt$. The induced vector potential $\mathbf{A}_{\text{ind}}(t)$ expresses the electric field caused by the polarization. Since the polarization is related to the average electronic current flowing in a unit cell, we have the following evolution equation for the induced vector potential:

$$\frac{d^2 \mathbf{A}_{\text{ind}}(t)}{dt^2} = \frac{4\pi}{c} \mathbf{i}(t), \quad (2)$$

where $\mathbf{i}(t)$ is the average electric current density in a unit cell, $\mathbf{i}(t) = \int_{\Omega} d\mathbf{r} \mathbf{j}(\mathbf{r}, t) / \Omega$, where Ω expresses the volume of the unit cell.

In practical calculations for a diamond, we take a cubic unit cell of eight carbon atoms and a lattice parameter of 6.74 a.u. We treat four valence electrons per atom by employing the norm-conserving pseudopotential of Ref. 24 for C^{4+} ion. The nonlocal part of the pseudopotential is treated in a separable approximation.²⁵ We employ the adiabatic local-density approximation (ALDA) for the exchange-correlation energy by using the functional form given in Ref. 26. The calculated small-amplitude response is in excellent agreement with a value for the static dielectric constant. The calculation also describes the absorption in the far UV quite well.¹⁹

We parametrize the time profile of the electric field from the laser pulse by $E_{\text{laser}}(t) = E_0 \sin^2(\pi t/T) \sin \omega t$ ($0 < t < T$). It is characterized by the maximum electric field E_0 , the frequency ω , and the pulse duration T . The time-dependent Kohn–Sham equations are solved in a uniform grid representation. The number of grid points is typically 18^3 , but finer grids are needed for laser pulses of lower frequency. The orbitals $\psi_i(\mathbf{r}, t)$ are specified by a band index n and a Bloch wave number \mathbf{k} , with 16^3 \mathbf{k} points representing each band. The time evolution is calculated with the Taylor expansion method of fourth order¹⁷ with a time step of $\Delta t = 0.02$ a.u. The total number of the time step is typically 50 000. We have carefully examined the convergence of the calculation with respect to three parameters, such as the grid spacing, the number of \mathbf{k} points, and the time step, in solving the TDKS equation.

We first show a typical time evolution in Fig. 1, where the laser pulse is characterized by the maximum laser intensity ($I_0 = 1 \times 10^{15}$ W/cm²), the laser frequency ($\hbar\omega = 3.1$ eV), and the pulse duration ($T = 40$ fs). Figure 1(a) shows the time profile of the electric field. The electric field of the applied laser pulse (blue dashed) and the total electric field (red solid) are compared. Figure 1(b) shows the number of excited electrons per carbon atom, which is defined by

$$n_{\text{ex}}(t) = \sum_{nn'\mathbf{k}} (\delta_{nn'} - |\langle \phi_{n\mathbf{k}} | \psi_{n'\mathbf{k}}(t) \rangle|^2). \quad (3)$$

Figure 1(c) shows the excitation energy per carbon atom as a function of time. In these figures, there occurs an abrupt and qualitative change in the electronic response around t

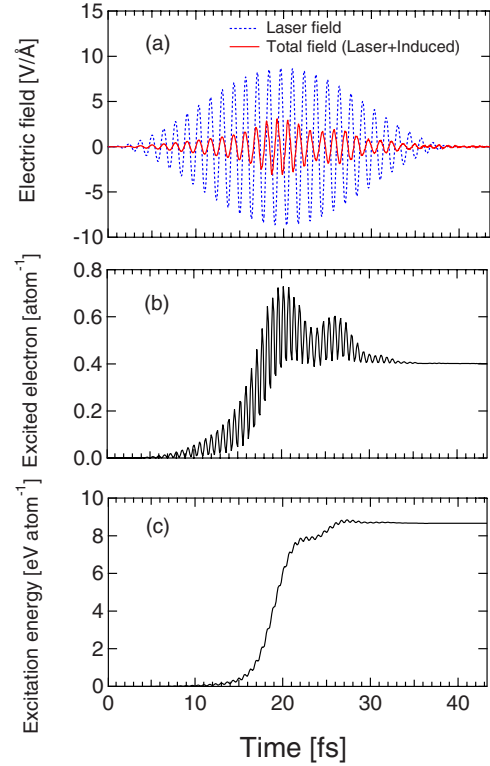


FIG. 1. (Color online) Electric field of an applied laser pulse (blue dashed curve) and the total electric field (red solid curve) are shown in (a) as a function of time. The applied laser pulse is characterized by a maximum intensity of 1×10^{15} W/cm², a pulse duration of 40 fs, and a laser frequency of 3.1 eV. The number of photoexcited electrons per carbon atom and the excitation energy per carbon atom are shown in (b) and (c), respectively.

$= 20$ fs. We consider that this change is a signature of the optical breakdown, as explained below.

At the initial stage of the laser pulse where the applied electric field is weak, the response is dielectric: The total electric field is proportional to the applied field, $E_{\text{tot}}(t) \approx \epsilon^{-1} E_{\text{ext}}(t)$, with the static dielectric constant of a diamond ($\epsilon \approx 6$). Starting at 15 fs, the number of excited electrons and the excitation energy undergo a rapid increase. Simultaneously, the total electric field starts to go out of phase with the applied electric field, signaling a large energy transfer. By about 20 fs, the applied and total electric fields are completely out of phase. At this point, the number of excited electrons and the excitation energy reach their saturation values. Note that the laser field is still strong during this entire time.

The physics of the later stage dynamics can be understood rather simply. Since there is no band gap for electrons excited into a conduction band, they may have a metallic response and produce a collective plasma oscillation. One may estimate the plasma frequency by

$$\omega_p = \left(\frac{4\pi n_{\text{ex}}}{m\epsilon} \right)^{1/2}, \quad (4)$$

where ϵ is the dielectric constant of a diamond. For the case shown in Fig. 1, the final number of excited electrons is 0.4

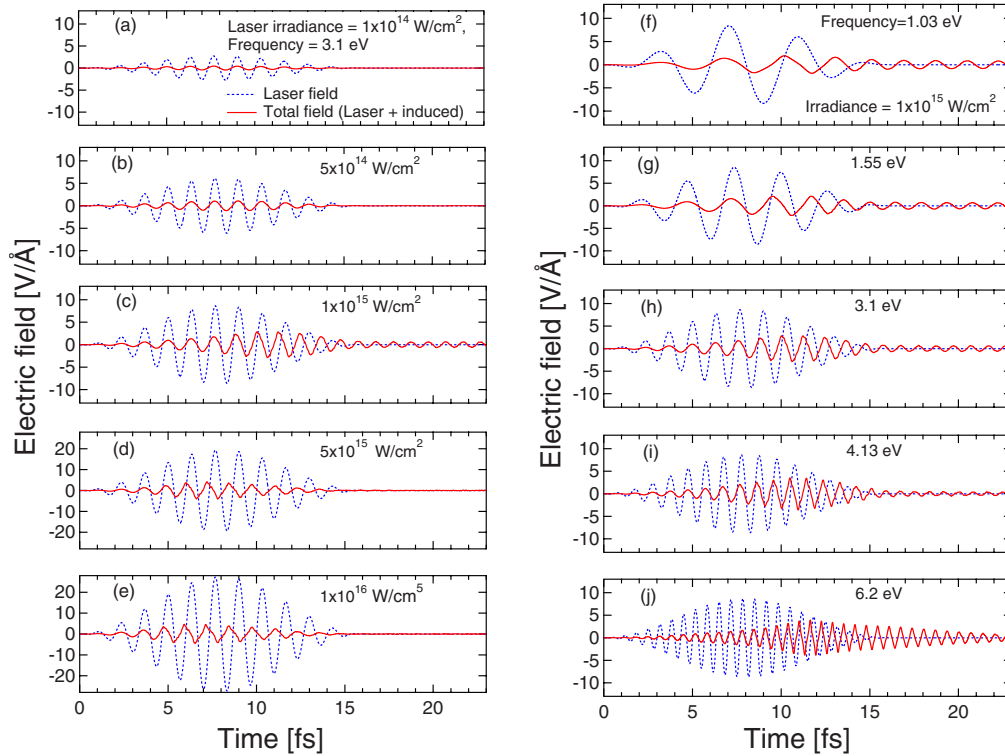


FIG. 2. (Color online) Electric fields of the applied laser pulse (blue dotted curve) and total electric fields (red solid curve) are shown as a function of time for different laser intensities and frequencies. (a)–(e) show the results of different laser intensities while the frequency is fixed at 3.1 eV. (f)–(j) show the results of different laser frequencies while the intensity is fixed at 1×10^{15} W/cm².

per carbon atom (0.7×10^{22} cm⁻³). The corresponding plasma frequency is $\hbar\omega_p = 4.0$ eV, which is slightly higher than the frequency of the applied laser pulse ($\hbar\omega = 3.1$ eV). This fact suggests the following scenario of the optical breakdown: As the intensity of the applied field increases, the electrons excited by perturbative and tunneling mechanisms slowly increase. When their density reaches a point such that the plasma and photon frequencies match, a resonant energy transfer occurs from the laser pulse to the electrons. This is when the optical breakdown takes place in the calculation. After the breakdown, the electrons in the conduction band screen the applied electric field and further energy transfer is suppressed.

Next, we examine how the breakdown depends on the intensity and frequency of the laser pulse. In all the calculations presented below, the pulse duration is fixed at $T = 16$ fs. Figures 2(a)–2(e) show the electric fields for cases in which the maximum laser intensity is varied, from 1×10^{14} to 1×10^{16} W/cm², while the frequency is fixed at $\hbar\omega = 3.1$ eV (corresponding to 400 nm wavelength). For $I_0 \leq 5 \times 10^{14}$ W/cm², the response is almost dielectric for the whole period. For $I_0 \geq 1 \times 10^{15}$ W/cm², a phase difference between the applied and total electric fields is observed. The phase deviation starts earlier for a larger laser intensity. In Fig. 2(c), one can see that the plasma oscillation continues long after the laser pulse ends. We have carefully examined the condition on which the oscillation appears and have found that it appears only when the dielectric breakdown occurs at the time between the middle and the end of the applied laser pulse. However, we have no explanation for this curious behavior.

In Figs. 2(f)–2(j), we show the effect of varying the frequency on the field, by covering the range from 1 to 6 eV. In these calculations, the peak intensity is fixed at 1×10^{15} W/cm². These figures show that the phase difference between the external and total electric fields occurs at around 10 fs in all cases. The occurrence of the optical breakdown thus principally depends on the intensity of the laser pulse and is less sensitive to the frequency.

In Fig. 2, we also observe that the oscillation of the total electric fields continues even after the applied laser pulse ends, irrespective of the laser frequency. The frequency of the oscillation is always higher than the frequency of the applied laser pulse. The oscillation shows a very small damping except in Fig. 2(j), where the laser frequency is 6.2 eV.

The oscillation in the total electric field after the applied laser pulse ends is a plasma oscillation of the electrons excited into a conduction band. Indeed, we confirmed that the frequencies of the oscillation seen in Figs. 2(f)–2(j) agree well with the plasma frequencies estimated by Eq. (4) with the number density of Eq. (3). The fact that the frequencies of the plasma oscillation are always slightly higher than the frequencies of the applied laser pulse may be naturally understood with our scenario of the optical breakdown. The plasma oscillation of conduction electrons may suggest an emission of a blueshifted light following the breakdown. This may be relevant to a supercontinuum emission, which is often observed in laser-material interactions.²⁷

Here, we examine the definition of the number of excited electrons. As seen in the middle panel of Fig. 1, $n_{\text{ex}}(t)$, as defined by Eq. (3), shows an oscillation as a function of time

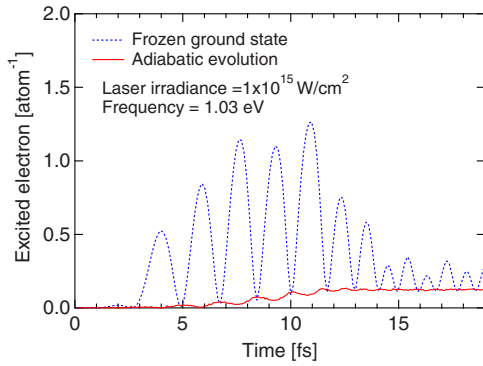


FIG. 3. (Color online) The number of excited electrons as a function of time is shown for a laser pulse of an intensity of 1×10^{15} W/cm², a pulse duration of 16 fs, and a frequency of 1.03 eV. Two curves are the results of Eq. (3) (blue dotted curve) and Eq. (6) (red solid curve).

when the laser pulse is applied. In Fig. 3, we show $n_{\text{ex}}(t)$ for the case of a laser pulse with $I_0 = 1 \times 10^{15}$ W/cm², $T = 16$ fs, and $\hbar\omega = 1.03$ eV by a blue dotted curve. The electric field in this calculation is shown in Fig. 2(f). In this case, the oscillation of the number of excited electrons as well as the oscillation of the induced vector potential persist even after the applied laser pulse ends. Therefore, $n_{\text{ex}}(t)$ defined by Eq. (3) may not be an appropriate definition for the number of excited electrons.

We have examined calculated results for various laser pulses and have found that the oscillation after the applied laser pulse ends depends on the total vector potential $\mathbf{A}_{\text{tot}}(t)$ with a dependence

$$n_{\text{ex}}(t) = n_0 + cA_{\text{tot}}(t)^2. \quad (5)$$

Here, the constant c is independent of the properties of the laser pulse. This fact suggests that the oscillation in $n_{\text{ex}}(t)$ may be an unphysical consequence of the gauge field.

This can be corrected by making a gauge-dependent definition of the ground-state orbitals. Let us consider a system whose ground state is described by the Bloch wave functions $\psi_{n\mathbf{k}}(t)$ and suppose that the slowly varying spatially uniform electric field described by a vector potential $\mathbf{A}(t)$ is applied. Then the orbitals may be adiabatically evolved by replacing the Bloch wave number \mathbf{k} with $\mathbf{k} + \mathbf{A}(t)$, $\psi_{n\mathbf{k}}(t) = \phi_{n\mathbf{k} + \mathbf{A}(t)}$. Since the whole \mathbf{k} region is occupied in the dielectrics, this adiabatic evolution does not produce any real excitation. However, $n_{\text{ex}}(t)$, as defined by Eq. (3), gives a finite number when $\mathbf{A}(t) \neq 0$. Therefore, the number of excited electrons should be calculated with respect to the evolved ground orbitals as

$$n_{\text{ex}}^{\text{ad}}(t) = \sum_{mn'\mathbf{k}} (\delta_{mn'} - |\langle \phi_{n\mathbf{k} + \mathbf{A}(t)} | \psi_{n'\mathbf{k}}(t) \rangle|^2). \quad (6)$$

In Fig. 3, the red solid curve shows the calculated number of excited electrons according to Eq. (6). Now the number of excited electrons is almost constant after the applied laser pulse ends.

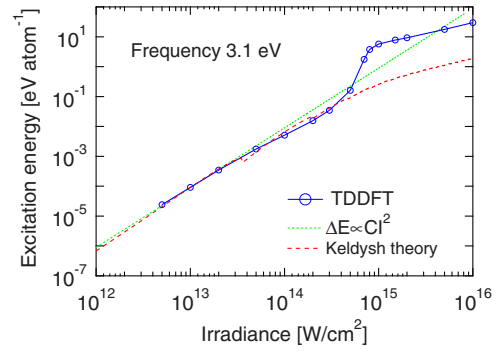


FIG. 4. (Color online) The energy deposited in a diamond by a laser pulse is shown as a function of intensity at a fixed laser frequency of 3.1 eV. The calculated values are shown by open circles connected by a blue line. A curve of $\Delta E \propto CI^2$ dependence is shown by a green dotted line. An estimation by the Keldysh theory (Refs. 11 and 29) is also plotted by a red dashed line. The curves of a quadratic dependence and of the Keldysh theory are normalized so that they coincide with the value of a real-time calculation at $I_0 = 5 \times 10^{12}$ W/cm².

In Fig. 4, we show the energy transfer in a diamond as a function of intensity. The laser frequency is fixed at 3.1 eV, which is larger than the calculated energy gap for a direct transition, (4.8 eV).²⁸ Since the applied laser frequency is smaller than the band gap, two photons are required for valence electrons to be excited across the band gap. Thus, we expect the energy transfer ΔE to depend on the laser intensity I as $\Delta E \approx CI^n$, with $n \approx 2$ in the multiphoton absorption picture. We show a curve of this dependence in Fig. 4 by a green dotted line. We also add by using a red dashed curve the rate by the Keldysh theory for a solid.^{11,29} The curves of quadratic dependence and of the Keldysh theory are normalized to the real-time calculation at the intensity of $I_0 = 5 \times 10^{12}$ W/cm². For a weak intensity region, a calculated energy transfer accurately follows the quadratic dependence. At intensities higher than 7×10^{14} W/cm², the energy transfer shows an abrupt increase. This behavior is consistent with the occurrence of a resonant energy transfer at the breakdown.

The calculated threshold for dielectric breakdown, 7×10^{14} W/cm² with 16 fs pulse, corresponds to 6 J/cm². The experimental threshold depends on the frequency and duration of the laser pulse, as well as the material,^{1,2,5,11,12} which is typically at a lower energy than that found here. In particular, the threshold for damage in a diamond has been measured at 0.63 ± 0.15 J/cm² for a 2 eV and a 90 fs pulse,³⁰ which is much lower than our calculation. It might indicate that the avalanche ionization is the process that determines the threshold. On the other hand, the pulses are subject to a self-focusing going through the material.^{6,8,12} This increases the effective field strength in local areas, allowing a higher threshold to be inferred from the profile of the laser beam. Further study seems to be needed before one can make a conclusion about the mechanism for optical breakdown.

Additional information about the excitation mechanism in TDDFT may be extracted from the distribution of electrons

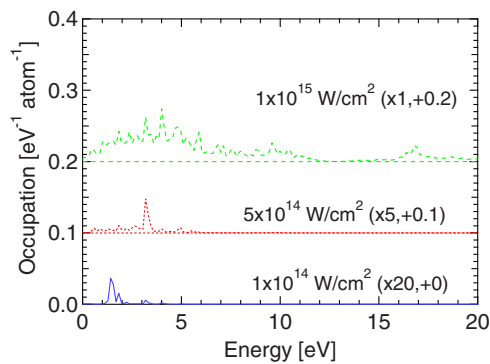


FIG. 5. (Color online) Occupation number distribution after the laser pulse ends. The intensities of the laser pulse are 1×10^{14} W/cm² (dashed) and 1×10^{15} W/cm² (solid). The laser frequency is fixed at 3.1 eV. The electron energy is measured from the bottom of the conduction band.

in the conduction band after the laser pulse ends. This is shown in Fig. 5 for several laser intensities at a fixed laser frequency (3.1 eV). At the laser intensities of 1×10^{14} and 5×10^{14} W/cm², the excited electrons show peaks at specific energies of 1.8 and 3.2 eV, respectively. We have confirmed that the particle-hole energies of these peaks coincide

with the energies of 2 and 3 photon absorptions, respectively. On the other hand, at the laser intensity of 1×10^{15} W/cm², where the optical breakdown occurs, the conduction electrons are broadly distributed in energy. After the laser pulse ends, the electron distribution does not change in our calculation. To describe a relaxation process toward the thermal distribution, we should incorporate an electron-electron collision process, which is not taken into account in the present TDKS equation with ALDA.

In summary, we have presented a methodology for an *ab initio* theory of electron dynamics in an insulator subject to an intense laser field. The theory, TDDFT, is seen to be capable of describing the optical breakdown phenomenon with a rather sharp threshold. This occurs in a diamond at around 7×10^{14} W/cm² with a pulse length of 16 fs. The optical breakdown is seen to be self-limiting due to plasma oscillations and screening by conduction band electrons. We have also found that the plasma oscillation may persist beyond the duration of the pulse.

This work is supported by the Grant-in-Aid for Scientific Research (Nos. 19019002, 18540366, and 17540231). The numerical calculation is achieved by Altix3700Bx2, JAEA, and by the massively parallel cluster PACS-CS, University of Tsukuba.

*Present address: Theoretical Nuclear Physics Laboratory, RIKEN Nishina Center, Wako 351-0198, Japan.

- ¹B. C. Stuart, M. D. Feit, A. M. Rubenchik, B. W. Shore, and M. D. Perry, Phys. Rev. Lett. **74**, 2248 (1995); B. C. Stuart, M. D. Feit, S. Herman, A. M. Rubenchik, B. W. Shore, and M. D. Perry, Phys. Rev. B **53**, 1749 (1996).
- ²M. Lenzner, J. Krüger, S. Sartania, Z. Cheng, C. Spielmann, G. Mourou, W. Kautek, and F. Krausz, Phys. Rev. Lett. **80**, 4076 (1998).
- ³D. Homoelle, S. Wielandy, A. L. Gaeta, N. F. Borrelli, and C. Smith, Opt. Lett. **24**, 1311 (1999).
- ⁴Y. Shimotsuma, P. G. Kazansky, J. Qiu, and K. Hirao, Phys. Rev. Lett. **91**, 247405 (2003).
- ⁵D. M. Simanovskii, H. A. Schwettman, H. Lee, and A. J. Welch, Phys. Rev. Lett. **91**, 107601 (2003).
- ⁶S. S. Mao, F. Quéré, S. Guizard, X. Mao, R. E. Russo, G. Petite, and P. Martin, Appl. Phys. A **79**, 1695 (2004).
- ⁷A. Vogel, J. Noack, G. Hüttman, and G. Paltauf, Appl. Phys. B: Lasers Opt. **81**, 1015 (2005).
- ⁸S. W. Winkler, I. M. Burakov, R. Stoian, N. M. Bulgakova, A. Husakou, A. Mermillod-Blondin, A. Rosenfeld, D. Ashkenasi, and I. V. Hertel, Appl. Phys. A **84**, 413 (2006).
- ⁹V. R. Bhardwaj, E. Simova, P. P. Rajeev, C. Hnatovsky, R. S. Taylor, D. M. Rayner, and P. B. Corkum, Phys. Rev. Lett. **96**, 057404 (2006).
- ¹⁰B. Rethfeld, Phys. Rev. Lett. **92**, 187401 (2004); Phys. Rev. B **73**, 035101 (2006).
- ¹¹A. C. Tien, S. Backus, H. Kapteyn, M. Murnane, and G. Mourou, Phys. Rev. Lett. **82**, 3883 (1999).
- ¹²A. Q. Wu, I. H. Chowdhury, and X. Xu, Phys. Rev. B **72**, 085128 (2005).
- ¹³J. L. Krause, K. J. Schafer, and K. C. Kulander, Phys. Rev. A **45**,

4998 (1992).

- ¹⁴S. Chelkowski, T. Zuo, and A. D. Bandrauk, Phys. Rev. A **46**, R5342 (1992).
- ¹⁵I. Kawata, H. Kono, and Y. Fujimura, J. Chem. Phys. **110**, 11152 (1999).
- ¹⁶E. Runge and E. K. U. Gross, Phys. Rev. Lett. **52**, 997 (1984).
- ¹⁷K. Yabana and G. F. Bertsch, Phys. Rev. B **54**, 4484 (1996).
- ¹⁸K. Yabana and G. F. Bertsch, Int. J. Quantum Chem. **75**, 55 (1999).
- ¹⁹G. F. Bertsch, J.-I. Iwata, A. Rubio, and K. Yabana, Phys. Rev. B **62**, 7998 (2000).
- ²⁰T. Nakatsukasa and K. Yabana, J. Chem. Phys. **114**, 2550 (2001).
- ²¹E. K. U. Gross, J. F. Dobson, and M. Petersilka, Top. Curr. Chem. **181**, 81 (1996).
- ²²F. Calvayrac, P.-G. Reinhard, E. Suraud, and C. A. Ullrich, Phys. Rep. **337**, 493 (2000).
- ²³T. Otobe, K. Yabana, and J.-I. Iwata, Phys. Rev. A **69**, 053404 (2004).
- ²⁴N. Troullier and J. L. Martins, Phys. Rev. B **43**, 1993 (1991).
- ²⁵L. Kleinman and D. M. Bylander, Phys. Rev. Lett. **48**, 1425 (1982).
- ²⁶J. P. Perdew and A. Zunger, Phys. Rev. B **23**, 5048 (1981).
- ²⁷A. K. Dharmadhikari, F. A. Rajgara, and D. Mathur, Appl. Phys. B: Lasers Opt. **80**, 61 (2005).
- ²⁸The experimental energy gap of a direct transition is about 7 eV, somewhat larger than the calculated one. This is a well-known deficiency of the commonly used energy functionals.
- ²⁹L. V. Keldysh, Sov. Phys. JETP **20**, 1307 (1965).
- ³⁰D. H. Reitze, H. Ahn, and M. C. Downer, Phys. Rev. **45**, 2677 (1992).